2024 IEEE International Symposium on Electromagnetic Compatibility, Signal & Power Integrity (EMC+SIPI) | 979-8-3503-6039-4/24/$31.00 ©2024 IEEE | DOI: 10.1109/EMCSIPI49824.2024.10705435

Modelling Weave effect in PCBs using 2D cross-sectional analysis

Dr. Victor Khilkevich
Dept. of Electrical and Computer Engineering – Electromagnetic Compatibility Laboratory
Missouri University of Science and Technology
Rolla, MO, USA
khilkevichv@mst.edu

Scott Hinaga
Cisco Systems Inc
San Jose, CA, USA
shinaga@cisco.com

***Abstract*— Printed circuit board dielectric substrates are composite materials produced by embedding fiber glass fabrics into epoxy resin. Because of this the medium in the PCB transmission lines is inhomogeneous which often leads to degradation of the signal integrity performance of the lines, particularly due to the differential skew. The detrimental effect of the fiber weave can be modeled relatively accurately using full-wave analysis, but at a high computational cost. Alternative modelling techniques are less demanding, but often lack accuracy. This article investigates a possibility of using the 2D cross-sectional analysis for the fiber weave effect modeling, which considerably decreases the computational cost of modeling while retaining the accuracy inherent to the field solvers.**

Keywords—PCB, weave effect, 2D cross-sectional analysis

I. Introduction

The weave effect in printed circuit boards (PCB) transmission lines (TL) draws considerable attention of electrical engineers [1].The most obvious manifestation of the wave effect is the dependency of the propagation delay on the position of the trace relative to the fiber bundles in the fabric [2] that in turn results in the differential skew limiting the TL performance [3]-[5]. The weave effect skew can significantly increase the insertion loss at frequencies as low as several GHz if the lines are long enough ([1], [4]).

The weave structure can be simulated in 3D [6], [7], but the resulting models are computationally expensive. Alternative approaches are approximated (for example, estimation of the substrate effective permittivity based on the volume fraction of glass and epoxy in [8], representation of the fiber glass inclusions as rectangular shapes in [9], and [10]) and might not produce required accuracy. The goal of this paper is to develop the weave effect modelling method combing the accuracy of the field solvers with computational efficiency.

II. Description of the method

A. 2D cross-sectional analysis and the PUL parameter calculation

Wave propagation in a translationally invariant transmission line (TL) is fully described by the per-unit-length (PUL) parameters of the line, which determine [11] the propagation constant

$$\gamma = \alpha + j\beta = \sqrt{(R + j\omega L)(G + j\omega C)} \tag{1}$$

and the characteristic impedance

$$Z_0 = \sqrt{\frac{R + j\omega L}{G + j\omega C}}, \tag{2}$$

where $R, L, G,$ and C are the PUL resistance, inductance, conductance, and capacitance of the line. The phase velocity of the wave is

$$v_p = \frac{\omega}{\beta}. \tag{3}$$

In general, both the characteristic impedance (2) and the phase velocity (3) depend on all four PUL parameters. However, for a practically important low-loss transmission line with $R \ll \omega L$ and $G \ll \omega C$, the effect of the loss terms becomes negligible, and the TL impedance and phase velocity can be calculated as

$$Z_0 \approx \sqrt{\frac{L}{C}}, \tag{4}$$

$$v_p \approx \frac{1}{\sqrt{LC}}. \tag{5}$$

Since the skew is produced due to the change of the phase velocity along the line with inhomogeneous dielectric, the lossless approximation appears to be sufficient to model the weave effect. In addition, the lossless condition simplifies the field equation formulation and allows to completely decouple the electric and magnetic equations.

The following formulation of the lossless 2D equations will be used henceforth [12]:

$$\nabla \cdot (\varepsilon \nabla \varphi) = 0, \tag{6}$$

$$\nabla \cdot \left(\frac{1}{\mu} \nabla \mathbf{A}\right) = 0. \tag{7}$$

where φ is the scalar electric potential, $\mathbf{A}$ is the vector magnetic potential (for a TEM mode the $\mathbf{A}$ vector is always perpendicular to the TL cross-section and equation (7) is actually a scalar equation similar to (6)), ε is the permittivity of the dielectric (a coordinate-dependent function for a line with inhomogeneous

Authorized licensed use limited to: Missouri University of Science and Technology. Downloaded on January 16,2025 at 18:43:51 UTC from IEEE Xplore. Restrictions apply.

dielectric), and μ is the permeability of the material (a constant equal to the vacuum permeability, assuming the TL materials are non-magnetic).

The excitation for both equations is specified by the potential difference at the boundaries of the conductors.

After the cross-sectional solution is found in potentials, the fields are calculated as

$$\mathbf{E} = -\nabla\varphi, \tag{8}$$

$$\mathbf{H} = \frac{1}{\mu}\nabla \times \mathbf{A}. \tag{9}$$

The PUL capacitance is then calculated as the ratio of the PUL charge to the potential difference between the conductors:

$$C = \frac{q}{V} = \frac{\oint_{\hat{c}} \varepsilon\mathbf{E}\cdot\mathbf{a}_n dl}{\varphi_2 - \varphi_1}, \tag{10}$$

where $\hat{c}$ is a contour encircling one of the conductors, $\mathbf{a}_n$ is the normal to that contour.

The PUL inductance is calculated as the ratio of the PUL magnetic flux to the current:

$$L = \frac{\psi}{I} = \frac{-\mu\int_a^{a'} \mathbf{H}\cdot\mathbf{a}_n dl}{\oint_{\hat{c}} \mathbf{H}\cdot\boldsymbol{dl}}, \tag{11}$$

where the integral in the numerator is calculated along a curve connecting the conductors (points a and a' lie on the conductor surfaces), $\mathbf{a}_n$ is the normal to the integration curve.

B. Modeling thanslationally varying transmission lines using 2D cross-sectional analysis

The premise of this paper is that it is possible to approximately model the transmission lines with non-translationally invariant cross-section by cutting it into segments short enough such that the geometrical variations withing the segments can be neglected, and then cascading the segments to represent the original geometry. The approach is inherently approximated, but under certain conditions segment cascading can produce satisfactory results. For example, in our previous publications [13], [14] it was shown that it is possible to model a microstrip with meshed ground plane quite accurately by analyzing its cross-sections. The approach presented in [13] and [14] required a modification of the PUL inductance of each segment due to the fact that the currents in the meshed ground can flow at an angle to the cross-section. The problem considered in this paper is even simpler compared to the previous one ([13], [14]) by the fact that the currents in the conductors are weakly disturbed by the dielectric non-uniformities and therefore the capacitance and inductance values obtained by the 2D analysis can be used without any modifications during cascading. A similar approach is used in [10], but with a drastic geometrical simplification allowing analytical calculation of the PUL capacitance. The presented method is free from this limitation.

The TL modelling is done by the following algorithm. The entire transmission line with the length l is divided into N short segments with the length $dz = l/N$. The values of the PUL capacitance C_i and inductance L_i for each segment are calculated as described in the previous section, and the ABCD matrices of segments are found:

$$ABCD_i = \begin{bmatrix} \cos\beta_i dz & jZ_i \sin\beta_i dz \\ \frac{j}{Z_i}\sin\beta_i dz & \cos\beta_i dz \end{bmatrix}, \tag{12}$$

where $\beta_i = \omega\sqrt{L_i C_i}$, and $Z_i = \sqrt{L_i/C_i}$.

The ABCD matrix of the complete line is found as a product:

$$ABCD = \prod_i ABCD_i = \begin{bmatrix} A & B \\ C & D \end{bmatrix}, \tag{13}$$

The transmission coefficient of the line S_{21} is determined by the ABCD to S-parameter conversion. And finally, the phase delay is calculated by differentiating the phase of the transmission coefficient with respect to the frequency:

$$\tau = -\frac{d\arg S_{21}}{d\omega}. \tag{14}$$

The 2D analysis described above was implemented in Matlab using Partial Differential Equation (PDE) toolbox.

C. Modelling of the transmission line geometry

The weave structure of the PCB transmission lines can be easily seen in cross-section. For example [15] demonstrates (Fig. 1) an image obtained by physically cutting a stripline perpendicular to the trace and imaging the cross-section using a scanning electron microscope (optical imaging is also possible). The characteristic shapes of the glass fabric bundles can be clearly seen in the picture (there is two layers of fabric above and two layers below the trace). The fabric layers are embedded into a resin compound and the boundaries between the two materials are clear.

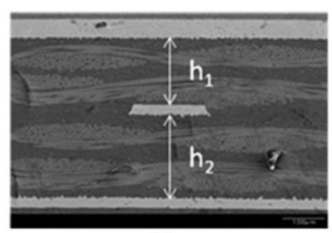

Fig. 1. Example of a stripline cross-section imaged by an SEM

Accurate modelling of the weave structure is important for textile industry and there are commercial tools capable of creating precise 3D weave models using mechanical FEM solvers (see [16] for example). Due to the unavailability of such tools to the authors, however, a simpler (and commonly used, see for example [7]) approach to the weave modelling was chosen. The trajectories of the weft and warp bundles of the fabric were modeled as sinusoidal functions (Fig. 2) and then the elliptical shapes were swept along the trajectories to represent the bundles. The bundles were considered uniform, such that the individual fibers were not modelled.

An example of the cross-section obtained using this model is given in Fig. 3. The cross-section generation algorithm is realized as a Matlab script.

Authorized licensed use limited to: Missouri University of Science and Technology. Downloaded on January 16,2025 at 18:43:51 UTC from IEEE Xplore. Restrictions apply.

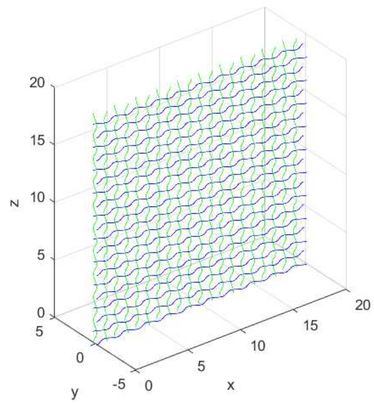

Fig. 2. Weft and warp bundle trajectories are represented by sinusoidal functions (dimensions are given in arbuitrary units)

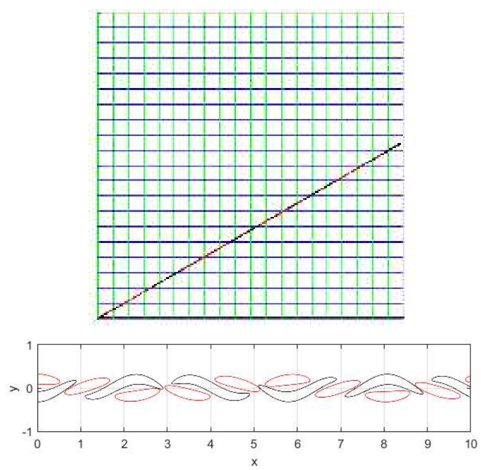

Fig. 3. Fiber bundle cross-section (bottom) taken along the line at 30 degrees relative to the x axis (top) (dimensions are given in arbuitrary units)

III. Validation of the propsed method on a simplified geometry

Strictly speaking, the 2D cross-sectional analysis can be used to characterize the translationally invariant transmission lines only. Any discontinuity in a TL will produce non-TEM fields that cannot be produced by a 2D solver. As such, application of the 2D analytic to non-translationally invariant lines inevitably introduces errors. However, the magnitude of these errors can be at an acceptable level (which is determined by the TL application), especially if the non-TEM fields due to discontinuities are relatively weak. We believe that this is exactly the case for practical PCB transmission lines where the substrate is a mixture of dielectrics with a relatively low permittivity contrast.

To test this hypothesis, a simplified geometry shown in Fig. 4 was simulated in a 3D solver (CST).

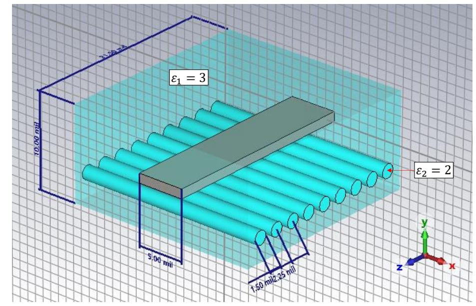

Fig. 4. A coaxial TL with non-uinform dielectric

The structure represented a coaxial waveguide with a rectangular central conductor and the bulk dielectric with permittivity of 3 (the outer conductor was formed by applying electric boundary conditions). Underneath the central conductor there was a series of dielectric cylinders with permittivity equal to 2 running perpendicular to the central conductor. The full-wave field analysis (Fig. 5) reveals that non-TEM z-component of the field is produced in the regions close to the cylinders. Its magnitude, however, is significantly (10-20 dB) lower than the magnitude of the dominant y-component.

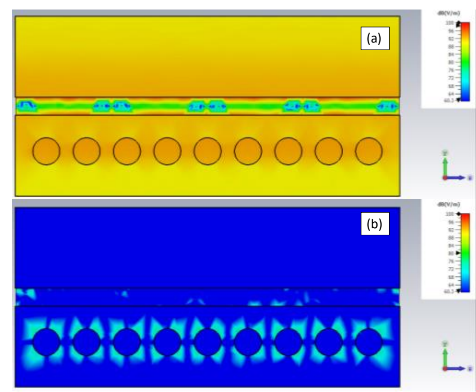

Fig. 5. Electric field at 10 GHz in the yz cross-section of the coaxial waveguide: (a) y-component, (b) z-component.

The y-component distribution, on the other hand, is noticeably distorted by the presence of the cylinders, and, what is important, the field is changed even in the gaps between the cylinders, which cannot be captured by the 2D analysis at all because the cross-section of the line between the cylinders is perfectly uniform. However, despite of these two effects, the phase delay curves calculated by the 2D analysis method described above and obtained as the results of the 3D solution agree very well up to at least 100 GHz (Fig. 6). Calculations for different values of the cylinder permittivity produce results with a similar level of accuracy.

The results obtained for the model in Fig. 4 demonstrate that the 2D analysis can be used to calculate the phase delay with a reasonably good accuracy despite its limitations.

Authorized licensed use limited to: Missouri University of Science and Technology. Downloaded on January 16,2025 at 18:43:51 UTC from IEEE Xplore. Restrictions apply.

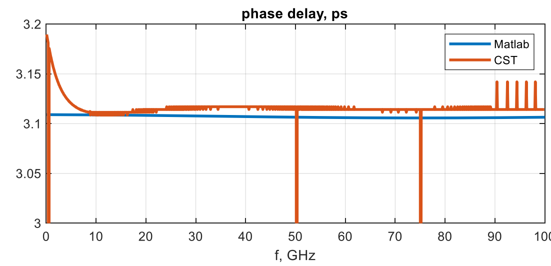

Fig. 6. Phase delay calculated by the 2D method (labeled "Matlab") and in full wave (labeled "CST")

IV. Modeling of the Transmission Lines with Glass Fabric Layers

The proposed method was applied first to a geometry presented in Fig. 7. The transmission line is formed by a rectangular central conductor (trace) surrounded by the rectangular outer shield (both are modelled as electric boundaries). The central conductor is surrounded by the bulk dielectric with permittivity $\varepsilon_1 = 3.3$ and there are two fabric layers below and above the trace with permittivity $\varepsilon_2 = 2$. The trace has the width of 11 mil. The distance to the "ground planes" is 10 mil. The trace is routed at 1 degree relative to the direction of the wrap bundles. The length of the transmission line is 1000 mil. The geometry is divided into 1000 segments with the length of 1 mil and the cross-sections of each segment are generated (Fig. 7 shows the cross-section of the first and last segments).

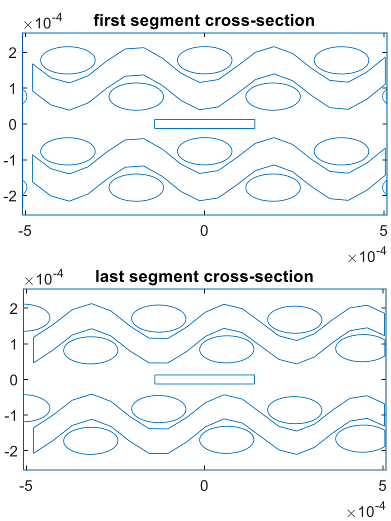

Fig. 7. Test geometry 1 (first and last segments). The dimensions are given in m; $5 \cdot 10^{-4}$ m is equal to 19.7 mil.

As the result of the calculation the impedances Z_i and propagation constants β_i of all segments are generated and the S-parameters of the line are calculated in the frequency range from 0 to 1500 GHz. The excessively high upper frequency was selected to investigate the reflection effects arising due to the periodicity of the fabric weave. Since the PUL L and C of the lossless line are frequency-independent, the frequency value affects (12) only and does not change the total calculation time.

It should be noted, however, that the results obtained at such high frequencies do not reflect the actual performance of the TL due to the neglect of loss and higher-order propagating modes in the model and should be used only for identification of the periodic discontinuities.

The phase delay and the magnitude of the transmission coefficient are shown in Fig. 8.

As can be seen the transmission line exhibits constant phase delay and transmission coefficient up to approximately 450 GHz, where a deep null in the transmission coefficient is observed. The null is produced by the reflection from the spatially periodic fiber bundles. Since the trace runs nearly perpendicular to the bundles which have a spatial period of 15 mills, the resonance frequency is very high.

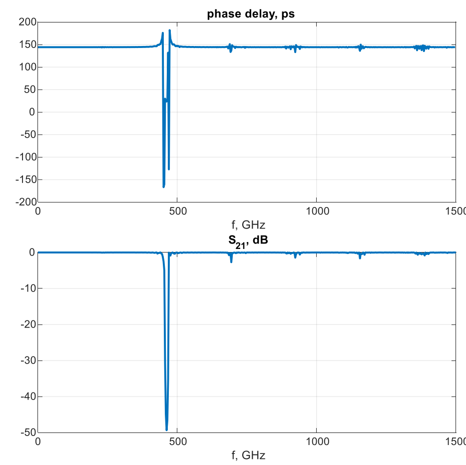

Fig. 8. Phase delay and magnitude of the transmission coefficient for Test geometry 1

The nulls in the transmission coefficient can be also identified by analyzing the spectrum of the characteristics impedance $Z(l)$, which depends on the coordinate along the trace of the transmission line l. By calculating the Fourier transform of $Z(l)$ and plotting its absolute value with respect to the half-wavelength frequency defined as

$$f_{\lambda/2} = \frac{v_p}{2T_{spatial}}, \quad (15)$$

where $T_{spatial}$ is the spatial period of the $Z(l)$ spectrum, the nulls in the fabric periodicities can be identified. An example of such calculation for the geometry in Fig. 7 is shown in Fig. 9.

As can be seen, the peeks of the $Z(l)$ spectrum perfectly match with the nulls in the transmission coefficient.

Another test geometry presented in Fig. 10 is a trace running at an angle of 15 degrees relative to the wrap bundles. The phase delay and the transmission coefficient of Test geometry 2 is presented in Fig. 11.

The phase delay is approximately the same in both test cases (see the angle sweep results in the next section for the numerical values), and the transmission coefficient are also similar with the main resonances around 450 GHz. However, the transmission coefficient of Test geometry 2 contains the resonances at lower

Authorized licensed use limited to: Missouri University of Science and Technology. Downloaded on January 16,2025 at 18:43:51 UTC from IEEE Xplore. Restrictions apply.

frequencies that can be seen directly in the transmission coefficient plot as well as in the spectrum of the characteristic impedance (Fig. 12).

Due to a significant angle between the trace and the fiber bundles a periodicity with a much longer period is observed in the characteristic impedance profile, resulting in the resonances at around 100 and 120 GHz, which potentially can create signal integrity issued for high-speed digital signals. The resonances are very weak for this particular geometry (the insertion loss in at the order of hundredths of a dB), and would not be of any practical concern, but the obtained results demonstrate the ability of the method to identify the weave effect resonances at any frequency of interest.

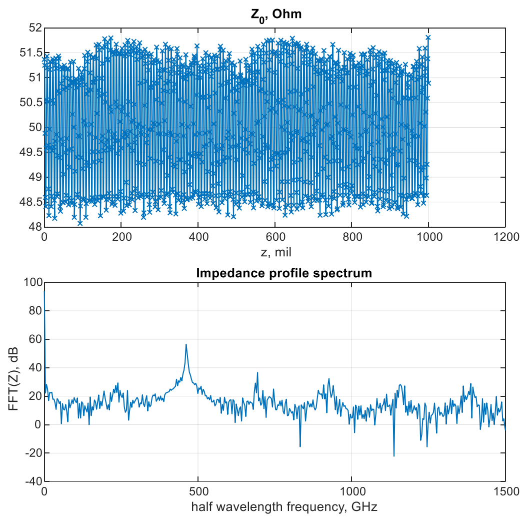

Fig. 9. Test geometry 1: characterisic impedance and its spectrum

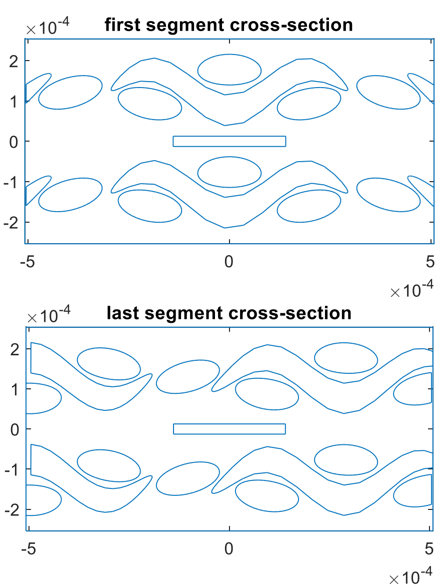

Fig. 10. Test geometry 2 (first and last segment). The dimensions are given in m; $5 \cdot 10^{-4}$ m is equal to 19.7 mil.

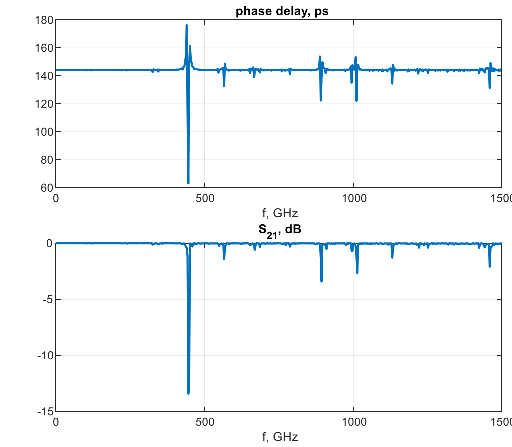

Fig. 11. Phase delay and magnitude of the transmission coefficient for Test geometry 2

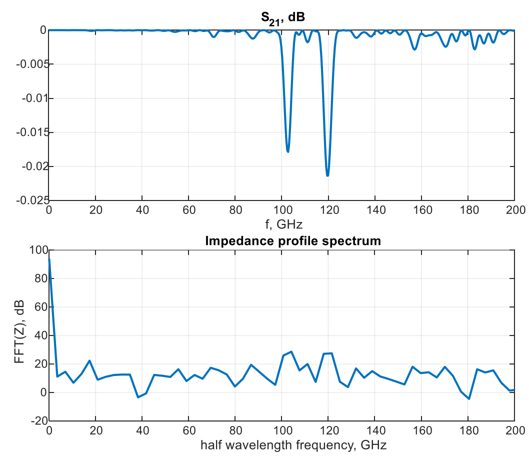

Fig. 12. Transmission coefficient and impedance spectrum for Test geometry 2 at lower frequencies

V. Computational Efficiency and Parameter Sweeps

Full-wave calculations of the fiber-glass dielectric are very computationally expensive and can require hours if long portions of the transmission lines are analyzed. Compared to this, the proposed method is very efficient. A single cross-section can be analyzed in several seconds (the exact number depends of course on the mesh count and the available computing power), however, since the cross-section calculations are completely independent, the solution time can be significantly reduced by taking advantage of parallelization, which opens possibilities to perform parameters sweeps and calculate, for example, the dependencies of the propagation delay on the position of the trace relative to the fiber bundles and its angle. The corresponding plots are presented in Fig. 13 and Fig. 14.

The calculations for Fig. 13 and Fig. 14 were performed on the Missouri S&T super computer The Foundry, which allowed up to 64 parallel threads in the Matlab code execution, resulting in tens of minutes of calculation time for the entire sweep. The

Authorized licensed use limited to: Missouri University of Science and Technology. Downloaded on January 16,2025 at 18:43:51 UTC from IEEE Xplore. Restrictions apply.

sweep results similar to Fig. 13 and Fig. 14 can be used to estimate, for example, the worst case of the differential skew and optimize the transmission line geometry. Such optimization might be impossible to perform with full-wave models of the glass fabric due to excessively long simulation times.

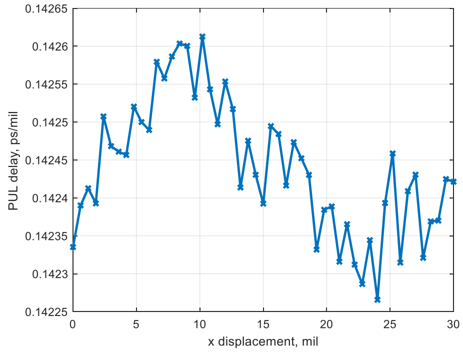

Fig. 13. PUL phase delay for the geometry in Fig. 10 as a function of the horizontal displacemen of the trace relative to the fabric.

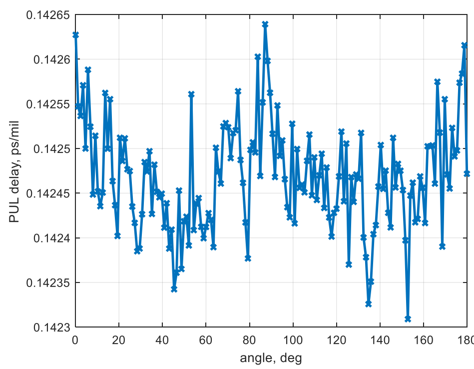

Fig. 14. PUL phase delay for the geometry in Fig. 10 as a function of the trace angle.

VI. Conclusions

A 2D algorithm for modeling the PCB transmission lines with glass fabric composite dielectrics is proposed. The algorithm was validated on a simplified structure and demonstrated good accuracy in terms of the phase delay. The computationally efficiency of the algorithm allows to perform simulation of long segments of transmission lines (several inches) in reasonable time by using parallelization of computations (for example, 1000 slices of geometry in Fig. 7 were analyzed in 82 seconds using 12 workers in Matlab's parallel pool). Short simulation time allows to perform parameter sweeps such as the position and angle of the trace relative to the fiber bundles as well as geometry optimizations.

It should be noted that the presented work is just a first step in the direction of the development of the accurate 2D algorithm for the weave effect modelling. Future steps will include more comprehensive validations against the fabricated PCBs and inclusion of the loss terms.

Acknowledgment

This work is supported in part by the National Science Foundation under Grants No. IIP-1916535 and No. OAC-1919789.

References

[1] J. Loyer, R. Kunze, X. Ye, “Fiber Weave Effect: Practical Impact Analysis and Mitigation Strategies,” White paper, Circuit tree.

[2] B. Chen, R. Yao, H. Wang, K. Geng, J. Li. “Effect of Fiber Weave Structure in Printed Circuit Boards on Signal Transmission Characteristics”. Applied Sciences. January 2019. 9(2):353

[3] H. Heck, S. Hall, B. Horine, K. Mallory and T. Wig, "Impact of FR4 dielectric non-uniformity on the performance of multi-Gb/s differential signals," Electrical Performance of Electrical Packaging, Princeton, NJ, USA, 2003, pp. 243-246.

[4] D. Bucur, "Fiber Weave Effect - a performance-limiting factor," 2014 10th International Conference on Communications (COMM), Bucharest, Romania, 2014, pp. 1-4.

[5] A. C. Durgun and K. Aygün, "Impact of fiber weaves on 56 Gbps SerDes interface in glass epoxy packages," 2015 IEEE 24th Electrical Performance of Electronic Packaging and Systems (EPEPS), San Jose, CA, USA, 2015, pp. 159-162.

[6] T. Fukumori, H. Nagaoka, D. Mizutani and M. Tani, "Simulation of differential skew considering fiber kink effects," IEEE CPMT Symposium Japan 2014, Kyoto, Japan, 2014, pp. 43-46.

[7] K. Nalla, A. Koul, S. Baek, M. Sapozhnikov, G. Maghlakelidze and J. Fan, "Measurement and correlation-based methodology for estimating worst-case skew due to glass weave effect," 2017 IEEE International Symposium on Electromagnetic Compatibility & Signal/Power Integrity (EMCSI), Washington, DC, USA, 2017, pp. 187-192.

[8] E. -K. Chua, J. -W. Zhang, K. -Y. See, W. -J. Koh and W. -Y. Chang, "Evaluation of fibre weaving of substrate on differential microstrip using an analytical approach," 2017 Asia-Pacific International Symposium on Electromagnetic Compatibility (APEMC), Seoul, Korea (South), 2017, pp. 350-352.

[9] C. -H. Wang, M. -T. Lu, J. -R. Huang, C. -S. Chen and R. -B. Wu, "Modeling and Mitigating Fiber Weave Effect Using Layer Equivalent Model and Monte Carlo Method," 2022 IEEE 72nd Electronic Components and Technology Conference (ECTC), San Diego, CA, USA, 2022, pp. 1851-1857.

[10] X. Tian et al., "Numerical investigation of glass-weave effects on high-speed interconnects in printed circuit board," 2014 IEEE International Symposium on Electromagnetic Compatibility (EMC), Raleigh, NC, USA, 2014, pp. 475-479.

[11] D. M. Pozar, Microwave Engineering. 2012 , John Wiley & Sons, Inc. Ch. 2

[12] C. Paul. Analysis of Multiconductor Transmission Lines. 2008. Wiley-IEEE Press. Ch. 2.

[13] Z. Sun et al., "Modeling of a Microstrip Line Referenced to a Meshed Return Plane," 2023 IEEE Symposium on Electromagnetic Compatibility & Signal/Power Integrity (EMC+SIPI), Grand Rapids, MI, USA, 2023, pp. 291-295.

[14] Z. Sun, J. Liu, X. Xiong, D. Kim, D. Beetner and V. Khilkevich, "Characterization of a Microstrip Line Referenced to a Meshed Return Plane Using 2-D Analysis," in IEEE Transactions on Signal and Power Integrity, vol. 3, pp. 13-20, 2024.

[15] M. Y. Koledintseva, A. V. Rakov, A. I. Koledintsev, J. L. Drewniak and S. Hinaga, "Improved Experiment-Based Technique to Characterize Dielectric Properties of Printed Circuit Boards," in IEEE Transactions on Electromagnetic Compatibility, vol. 56, no. 6, pp. 1559-1566, Dec. 2014.

[16] DFCA Digital Fabric and Composite Analyzer, Accessed: Jan. 07, 2024. [Online]. Available: https://fabricmechanics.com/

Authorized licensed use limited to: Missouri University of Science and Technology. Downloaded on January 16,2025 at 18:43:51 UTC from IEEE Xplore. Restrictions apply.